

Explore as a Storm, Exploit as a Raindrop: On the Benefit of Fine-Tuning Kernel Schedulers with Coordinate Descent

MICHAEL CANESCHE, UFMG, Brazil

GAURAV VERMA, Stony Brook University, USA

FERNANDO MAGNO QUINTÃO PEREIRA, UFMG, Brazil

Machine-learning models consist of kernels, which are algorithms applying operations on tensors—data indexed by a linear combination of natural numbers. Examples of kernels include convolutions, transpositions, and vectorial products. There are many ways to implement a kernel. These implementations form the kernel’s optimization space. Kernel scheduling is the problem of finding the best implementation, given an objective function—typically execution speed. Kernel optimizers such as AnsoR, Halide, and AutoTVM solve this problem via search heuristics, which combine two phases: exploration and exploitation. The first step evaluates many different kernel optimization spaces. The latter tries to improve the best implementations by investigating a kernel within the same space. For example, AnsoR combines kernel generation through sketches for exploration and leverages an evolutionary algorithm to exploit the best sketches. In this work, we demonstrate the potential to reduce AnsoR’s search time while enhancing kernel quality by incorporating Droplet Search, an AutoTVM algorithm, into AnsoR’s exploration phase. The approach involves limiting the number of samples explored by AnsoR, selecting the best, and exploiting it with a coordinate descent algorithm. By applying this approach to the first 300 kernels that AnsoR generates, we usually obtain better kernels in less time than if we let AnsoR analyze 10,000 kernels. This result has been replicated in 20 well-known deep-learning models (AlexNet, ResNet, VGG, DenseNet, etc.) running on four architectures: an AMD Ryzen 7 (x86), an NVIDIA A100 tensor core, an NVIDIA RTX 3080 GPU, and an ARM A64FX. A patch with this combined approach was approved in AnsoR in February 2024. As evidence of the generality of this search methodology, a similar patch, achieving equally good results, was submitted to TVM’s MetaSchedule in June 2024.

1 INTRODUCTION

A *kernel* is an algorithm that applies operations on *tensors*: chunks of memory indexed by a linear combination of natural numbers. A *Tensor Compiler* is a compilation infrastructure that generates code for kernels. As Ansel et al. [2024] explains, many tensor compilers, including TVM [Chen et al. 2018], nvFuser [Sarofeen et al. 2022] and NNC [Zolotukhin 2021], follow a design probably inspired by Halide [Ragan-Kelley et al. 2013]. These compilers separate the kernel’s semantics (what the kernel does) from its schedule (when the kernel does it). Since the same kernel semantics can be implemented in many different schedules, tensor compilers face a challenge called *kernel scheduling*: determining a suitable ordering for the operations a kernel performs on tensors. Kernel scheduling is typically addressed via heuristics because the *Kernel Optimization Space*—the set of all implementations of a kernel—is extremely vast, as Li et al. [2021] explains.

The Apache TVM tensor compiler employs three distinct optimization infrastructures for solving kernel scheduling: AutoTVM [Chen et al. 2018], AnsoR [Zheng et al. 2020] and MetaSchedule [Shao 2021]. AutoTVM finds parameters of *kernel sketches*. The sketch of a kernel represents the optimizations applied to the abstract description of that kernel, such as loop unrolling, splitting, interchange, and tiling. Many of these optimizations are parameterizable. Examples of parameters include the unrolling factor in loop unrolling and the width of the tiling window in loop tiling. AutoTVM assigns values to these parameters using various search heuristics. One of these heuristics is of interest in this paper: Droplet Search [Canesche et al. 2024]. Droplet Search seeks the optimal configuration

of an optimization template by determining a descent direction along the objective function that models the running time of the kernel. AnsoR and MetaSchedule (in contrast to AutoTVM) have the capability to generate new sketches. In other words, these schedulers are not restricted to a single sequence of optimizations. Section 2.1 provides further details on how AnsoR works, whereas Section 2.2 explains how Droplet Search works.

A Combined Search Infrastructure. Both AnsoR and MetaSchedule typically generate higher-quality kernels compared to AutoTVM’s Droplet Search, as they are not limited to a single search space. Each new sketch leads to the exploration of an entirely new search space. However, when constrained to a single sketch, Droplet Search tends to outperform these schedulers. Drawing on the terminology from recent work by Ding et al. [2023], Droplet Search’s coordinate descent approach is “*hardware centric*”, while AnsoR’s genetic algorithm is “*input centric*”; better embodying this quality that Sorensen et al. [2019] calls “*performance portability*”. In essence, Droplet Search, by traversing the search space contiguously, is sensitive to cache sizes and levels in the cache hierarchy. Nevertheless, despite Droplet Search’s tendency to identify optimal points within the search space, this algorithm is unable to navigate beyond this space due to its reliance on the initial sketch.

Inspired by these observations, this paper addresses the following research question: “*Is it possible to combine the wide exploration phase of AnsoR¹ with Droplet Search’s exploitation; thus, obtaining the advantages of each approach?*” By doing so, we can develop a version of AnsoR that produces superior kernels compared to the original tool while also reducing search times. This paper brings evidence that such a combination is effective. The core idea presented in this work is as follows: Initially, we allow AnsoR to explore the kernel optimization space, leveraging its “space travel ability” to test different sequences of optimizations during this exploration. Subsequently, following this initial exploration phase, we identify the most promising kernel space discovered by AnsoR and employ AutoTVM’s Droplet Search—a line search algorithm—to find a good kernel within this space.

Summary of Findings. This paper describes findings of an eminently empirical nature. The search techniques discussed in Section 2 are not an original contribution of this work: AnsoR’s exploration algorithm was designed by Zheng et al. [2020], and Droplet Search was incorporated into AutoTVM by Canesche et al. [2024], and further explored by Li et al. [2024]. Nevertheless, combining these two techniques into a practical tool required a number of experimental observations and engineering decisions, which Section 3 organizes into six research questions.

The new search methodology that emerged out of this combination has been considered sufficiently practical to be approved into Apache TVM. A request for comments was submitted to the TVM community in December of 2023, and a patch was approved into AnsoR in February of 2024. The patch has not yet been merged into an official release of TVM at the time of this submission. We have, subsequently, incorporated a coordinate descent exploitation phase into MetaSchedule [Shao 2021], which uses different search algorithms than AnsoR. These results are even better than those observed in AnsoR. Consequently, a new request for comments was submitted to the TVM community in June 2024, together with a patch for MetaSchedule [Canesche 2024].

The experiments in Section 3 show that the combined exploration-exploitation methodology outperforms the original implementation of AnsoR in terms of kernel quality and search speed. Positive results are reported in four different processors (AMD R7-3700X, Fujitsu ARM A64FX, NVIDIA RTX 3080, and NVIDIA A100), and in 20 popular deep-learning models, including AlexNet, VGG, ResNet, MobileNet, Inception, GoogLeNet, and DenseNet. As an illustration, by terminating AnsoR after sampling 300 kernels and then optimizing the best candidate with Droplet Search, we

¹This paper uses AnsoR as the basis for experiments; however, similar results have been reproduced in the MetaSchedule [Canesche 2024]. We focus on AnsoR because it is documented in an academic work [Zheng et al. 2020].

outperformed Ansor running with a budget of 10,000 samples in all the 4×20 architecture-model pairs. For instance, the combined search approach, on MnasNet, yields kernel speedups of 1.59x, 1.02x, and 1.08x on x86, ARM, and NVIDIA platforms, respectively. The search time for the combined approach correspondingly decreases by 1.25x, 1.25x, and 1.18x on these architectures.

2 EXPLORATION VIA ANSOR; EXPLOITATION VIA DROPLET SEARCH

A kernel is an abstract concept: it can be represented by operations on memory indexed by a linear combination of natural numbers. The actual implementation of a kernel is determined by its *schedule*. The schedule of a kernel determines in which order the different memory elements are accessed when the kernel runs. Following the terminology introduced in the original Ansor work [Zheng et al. 2020], a schedule is the combination of two notions: a *sketch* and an *annotation* of the sketch. Definition 2.1 enumerates these notions.

Definition 2.1 (The Kernel Search Space). The naïve implementation of a kernel replaces each linear index in the abstract representation of the kernel with a loop. A sketch is a sequence of transformations, such as loop fusion, splitting, or tiling, that can be applied to the naïve implementation of the kernel. An annotation of the sketch is the set of parameters that control the effect of each optimization in the sketch, such as unrolling factor, length of tiling window, number of threads in parallelization, etc. We call an annotated sketch a “kernel”. A kernel is a concrete program: it effectively runs. Each sketch determines a kernel search space, which is the set of every valid way to annotate that sketch.

Example 2.2. Figure 1 (a) shows an example of an abstract kernel. Figure 1 (b) shows a naïve implementation of the abstract kernel seen in Figure 1 (a). Figure 1 (c) shows two sketches produced after the application of different code optimizations onto the program in Figure 1 (b).

<p>(a) $C[i, j] = \sum_k A[i, k] \times B[k, j]$</p> <p>$D[i, j] = \max(C[i, j], 0)$</p> <p>where $0 \leq i, j, k \leq 512$</p>	<p>(c-i) parallel i.0@j.0@i.1@j.1 in range(P0): for k.0 in range(P1): for i.2 in range(P2): unroll k.1 in range(P3): unroll i.3 in range(P4): vectorize j.3 in range(P5): C[...] += A[...] * B[...]</p> <p>for i.4 in range(P6): vectorize j.4 in range(P7): D[...] = max(C[...], 0.0)</p>	<p>(d-i) P0 = 256 P1 = 32 P2 = 16 P3 = 16 P4 = 4 P5 = 16 P6 = 64 P7 = 16</p>
<p>(b) for i in range(512): for j in range(512): for k in range(512): C[i, j] += A[i, k] * B[k, j]</p> <p>for i in range(512): for j in range(512): D[i, j] = max(C[i, j], 0.0)</p>	<p>(c-ii) parallel i.2 in range(P8): for j.2 in range(P9): for k.1 in range(PA): for i.3 in range(PB): vectorize j.3 in range(PC): C[...] += A[...] * B[...]</p> <p>parallel i.4 in range(PD): for j.4 in range(PE): D[...] = max(C[...], 0.0)</p>	<p>(d-ii) P8 = 16 P9 = 128 PA = 512 PB = 32 PC = 4 PD = 512 PE = 512</p>

Fig. 1. (a) Abstract view of a kernel. (b) Naïve implementation of the abstract kernel. (c) Two optimization sketches for the naïve kernel. (d) Different annotations for the sketches.

Figure 1 (d) shows different parameters of the sketches in Figure 1 (c). As introduced in Definition 2.1, the set of every valid configuration of annotations for a given sketch forms the *search space* of that sketch. This space has one dimension for each parameter that is allowed to vary. Figure 2 shows two views of the optimization space of the two sketches in Figure 1 (c).

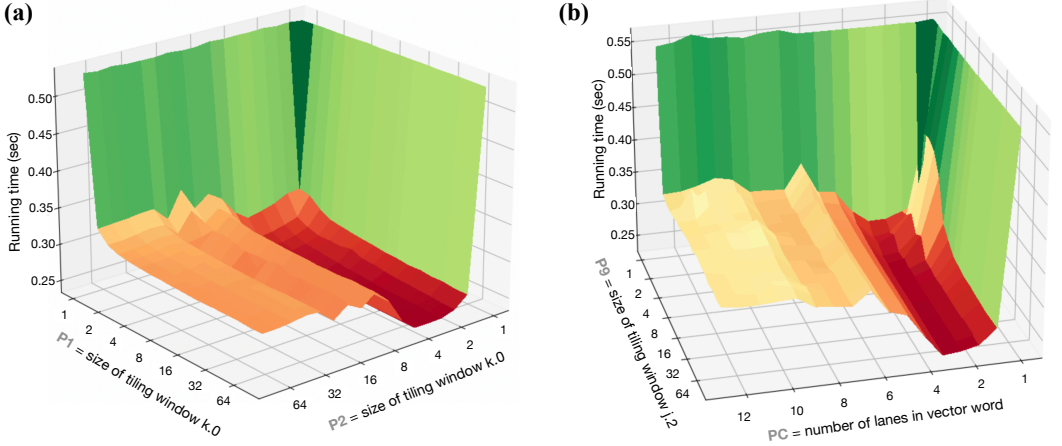


Fig. 2. (a) A three-dimensional view of the optimization space formed by the parameters **P1** and **P2** seen in Figure 1 c-i. (b) A three-dimensional view of the optimization space of parameters **P9** and **PC**.

2.1 Space Exploration via Ansor

Ansor solves kernel scheduling in an interactive process that involves three phases:

- Sketch generation:** in this phase, new sketches are created. As explained in Definition 2.1, each sketch determines one kernel search space.
- Sketch annotation:** in this phase, an initial population of annotated sketches is created. Following Definition 2.1, each annotated kernel is a point in the search space determined by the sketch that provides the annotations.
- Kernel evolution:** in this phase, candidate kernels are sorted according to an estimation of their performance (via Ansor’s cost model). The best candidates are sampled (executed and timed), and this information is used to improve the cost model.

Sketch Generation. The generation of new sketches happens via the application of a small collection of rewriting rules, which Figure 3 enumerates². Each rewriting rule provokes a code transformation, such as tiling, parallelization, or unrolling. The sketch generation rules are hardware-dependent: some rules, like those that bind loop iterations to threads, are only well-defined for GPUs, for instance. Notice that in addition to the rules seen in Figure 3, users can still add custom rules to the set of available sketch transformations.

Example 2.3. Figure 4 (a) shows a variation of the sketch earlier seen in Figure 1 (b). Each loop has an unrolling factor, which will have to be annotated in the initialization phase of the autotuning process. Figure 4 (b) shows an application of the “Always inlining” rule onto Figure 4 (a). It is important to note that neither of these program representations qualifies as a “kernel”, since they are not executable. To transform them into concrete kernels, the annotation within the unrolling factor must be assigned an actual value.

²Rules implemented in https://github.com/apache/tvm/tree/main/src/auto_scheduler/search_policy on 02/01/2024

Skip state	This rule is the identity function, which does not modify the current kernel. Its existence allows more flexibility to define rewriting rules, as they do not need to have all the same number of transformations.	Add cache write	Write data into the cache, e.g., as a way to support data layout transformations such as split, fuse and multi-level tiling.
Always inlining	This rule implements a variation of classic loop fusion (although called 'inline'). Given two loops, L1 and L2, where the former produces data that the latter consumes (without loop carried dependencies), the "inlining" operation merges these two loops.	Add reduction factor (rFactor)	This rule implements a loop as a reduction whenever such is possible, which can be run in parallel. In this case, the reduction operation (e.g.: add, mul or max) must be associative.
Multi-level tiling	This rule divides a nest of loops into various levels of subloops to enhance data locality. The goal of tiling is to arrange together data that are likely to be accessed in operations that are close in time.	Cross thread reduction	This rule determines the reduction factor for the reduction operators if they are not an intermediate stage created by cache write and there is sufficient parallelism. It also verifies the kernel fusibility and executes split and bind transformations accordingly.
Simplify tensor	This rule unrolls the indices of constant tensors or tiles that have a default tile level set to 2.	Add cache read	This rule, meant for GPUs, moves data from local to shared memory. The shared memory provides much faster access than local memory. Data is brought into shared memory by independent threads in parallel.
Multi-level tiling with fusion	This rule combines different loops in a transformation with cache-write, if the hardware supports it. It then executes multi-level tiling on the fused loops.	Special compute location	This rule identifies the unrolled outer space iterator and applies some specified transformation to compute at a designated location.

Fig. 3. Sketch generation rules. Ansoor uses these rules to change the kernel search space. Each rule modifies a sketch, e.g., fusing, splitting or tiling loops. However, these rules do not change the annotations in the sketch.

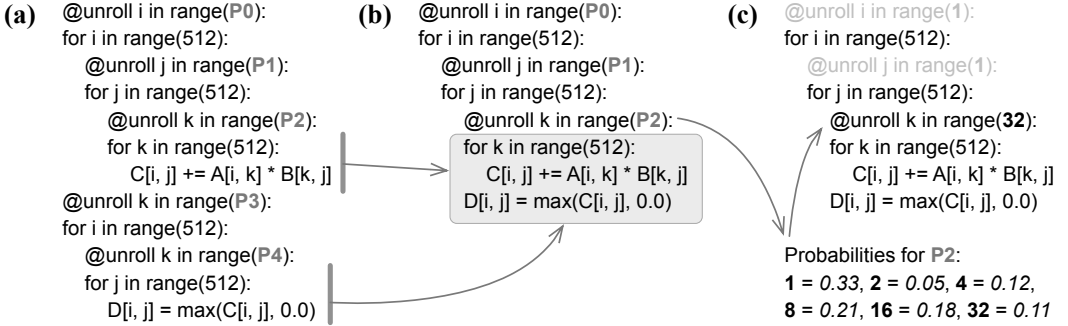


Fig. 4. (a) Sketch of the abstract kernel seen in Figure 1 (a). (b) Sketch that ensues from the application of the "Always inlining" rule. (c) Sketch that ensues from the initialization of the unrolling factor.

The Initialization of Annotations. Sketches are not executable programs: they have annotations which must be replaced with actual values. These values are the parameters of optimizations, as Definition 2.1 explains. Thus, as a second step of the iterative exploration approach of Ansoor, an initial population of annotated sketches is produced via the application of "initialization rules". Figure 5 summarizes the rules available in Ansoor at the time this work was produced. Each initialization rule is parameterized by a probability distribution, which associates concrete values with the probability that they can be chosen. Example 2.4 shows how these distributions are used.

Example 2.4. Figure 4 (c) shows the concrete kernel that comes out of the application of the "Unroll" rule (in Figure 5) to the sketch in Figure 4 (b). Figure 4 (c) also shows the probability distribution used to randomly choose the initial unrolling factor of 32.

Evolution of the Annotated Sketch. To explore different kernel spaces, Ansoor keeps a population of promising *candidate kernels*. This population is updated in an iterative process. At each iteration,

Fill tile size	This rule randomly assigns tile sizes to all tiled loops.	Unroll	This rule randomly assigns unrolling factors to the loops marked to be unrolled.
Vectorize	This rule combines and vectorizes iterations of the innermost loop. It is only applicable if memory accesses are contiguous across loop iterations.	Parallel	This rule fuses and parallelizes outermost loops. It stops upon finding reduction operations, or if the parallel annotation exceeds 16x the number of cores.
Change compute location	This rule skips all inlined, placeholder, and tiled loops. Then, it employs a random choice (0, 1, 2) to determine where computations will run.	Bind	This rule binds SIMD thread identifiers to loop iterations. By mapping computations to separate threads, the bind operation implements parallelization in graphic processing units.

Fig. 5. Rules that Ansoor uses to create an initial population of kernels, which will be the starting point to the evolutionary search.

Tile size	This rule evaluates a tiling window and increases its length. The rule ensures that the increase is less than the maximum innermost split factor and conducts permutations of the tile size accordingly.	Auto parallel	This rule applies in a scenario where parallelism was added to the outermost loop, and this loop was generated by fusing outer loops. One loop in the nest is randomly selected from all the parallel loops, and a parallelism factor is chosen for it.
Compute location	This rule assigns a given transformation step to a different computing device than all the previous locations used in that computation.	Auto unroll	This rule changes the unrolling factor of a loop marked to be unrolled. It uses the previous history of that unrolling location to determine the new factor.

Fig. 6. Mutation rules for evolutionary search. In contrast to the initialization rules seen in Figure 5, the mutation rules take the history of previous annotations when determining the next value of a given annotation.

the current population of candidates evolves through the application of the mutation strategies enumerated in Figure 6. To select the next set of candidates, Ansoor does not run every kernel in the current population. Instead, it uses a cost model to select candidates that are likely to run efficiently. These promising candidates are executed, and the result of these samples is used to recalibrate the cost model; hence, improving the estimates of the next candidates. Periodically, the algorithm reports statistical information regarding the search progress, including maximum and minimum scores, population size, and mutation success rates. Upon completion of the specified number of iterations, the best-performing kernels are recorded as the output.

Termination in Ansoor. The number of possible schedules is very large; hence, Ansoor limits the amount of schedules with a *budget of trials*. Each trial consists of the observation of the execution of an actual schedule, which happens at the end of the evolutionary phase. Because a machine learning model contains many kernels, an initial round of trials is partitioned among these layers. Layers are grouped into a worklist, and receive a quota of trials in round-robin fashion. After an initial round of optimizations, layers that run for a very short time are removed from this worklist. This process ensures that layers that run for the longest time are subject to more extensive optimizations. This approach is what Zheng et al. [2020] call “optimizing with gradient descent”. Because the budget of trials is fixed, Ansoor is guaranteed to terminate.

Limitations of Ansoor. The main limitation of Ansoor is the fact that it is oblivious to the structure of the search space. For instance, if we observe a performance improvement by increasing the unrolling factor of a loop from 4 to 6, it is likely that if we increase it further to 8, another improvement will also be observed. However, if going to 8 results in performance degradation, then further increases are likely to not bring improvements either. Ansoor’s exploitation approach, via an evolutionary algorithm, is not aware of this notion of neighborhood between kernels or of potential convex regions in the optimization space.

2.2 Space Exploitation via Droplet Search

Droplet Search [Canesche et al. 2024] is a kernel scheduling algorithm available in AutoTVM. AutoTVM differs from Ansor because it does not create new sketches. Rather, it is restricted to modifying the parameters of a single sketch—the *origin* of the optimization space. AutoTVM provides several independent scheduling approaches: random sampling, grid sampling, genetic sampling, etc. However, only Droplet Search will be of interest to this presentation³. Droplet Search is a variation of an exploitation algorithm called *Coordinate Descent*⁴. It relies on the premise that the parameters of a sketch can be arranged into a coordinate space. Figure 7 contains an annotated version of the algorithm.

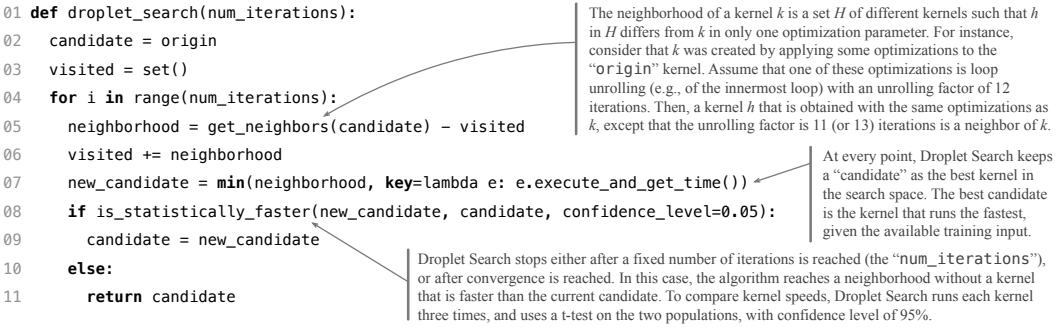


Fig. 7. The Droplet Search kernel scheduling algorithm. This pseudo-code is a simplified version of the original presentation of the algorithm, taken from [Canesche et al. 2024]. We have removed speculation and parallelism from this version as these features are immaterial for the presentation of our ideas.

Example 2.5. Let us assume a sketch formed by two optimizations: unrolling and tiling. For the sake of this example, unrolling supports five “unrolling factors”: $\{1, 2, 3, 4, 5\}$. These are the parameters of the loop unrolling optimization. Tiling is parameterized by the size of the tiling window. Let us assume the following sizes: $\{1, 2, 4, 8, 16\}$. The optimization space, in this case, is formed by 5×5 points, such as $(1, 1)$, which means no optimization, or $(3, 16)$, which indicates that the loop must be unrolled three times, and then tiled with a window of size 16. These points, e.g., $(1, 1)$, $(3, 16)$, etc, are the *coordinates* of the optimization space.

From the notion of coordinates, Droplet Search defines a *neighborhood function*: a function that returns the *neighbors* of a given coordinate. Intuitively, the neighbors of a coordinate are the points that are the closest to it. In Example 2.5, the neighbors of $(\text{unrolling} = 3, \text{tiling} = 8)$ would be the points $(2, 8)$, $(4, 8)$, $(3, 4)$ and $(3, 16)$. From this concept of neighborhood, Droplet Search works iteratively as follows:

- (1) At iteration zero, let the best current candidate be the set of parameters that implement no optimization.
- (2) Let (c_1, c_2, \dots, c_n) be the best set of parameters discovered up to iteration i .
 - (a) If there exists $c'_i, 1 \leq i \leq n$, such that $(c_1, \dots, c'_i, \dots, c_n)$ yields a faster kernel than $(c_1, \dots, c_i, \dots, c_n)$, then update the current best candidate to use c'_i instead of c_i .
 - (b) If there is no such c'_i , then the search terminates.

³Section 3.4 shall compare Droplet Search with the other techniques available in AutoTVM as when they are used as Ansor’s exploitation mechanism.

⁴It is unclear who invented Coordinate Descent. Descriptions of the algorithm can be found in classic textbooks [Zangwill 1969]. For a comprehensive overview, we recommend the work of Wright [2015].

Limitations of Droplet Search. Droplet search is a fast search algorithm when compared to Anzor or to other approaches available in AutoTVM [Canesche et al. 2024]. However, it has two fundamental limitations:

- Droplet Search is restricted to a single sketch. In other words, it can modify a sketch’s annotations, but it cannot create new sketches. This is a limitation of any search algorithm used in AutoTVM, but it is not a limitation of Anzor.
- Droplet Search depends highly on the initial schedule it receives as the *seed* of the search procedure. If this initial schedule does not exist in the same convex region as the optimal schedule, then Droplet Search cannot find the optimal schedule.

By combining Anzor and Droplet Search, we hope to circumvent the limitations of both search techniques. Section 2.3 explains how these two approaches can be used together.

2.3 Combining Anzor with Droplet Search

To combine Droplet Search and Anzor, we determine two parameters:

- K : the budget of trials of Anzor.
- $N < K$: a subset of trials.

We then proceed as follows:

- (1) Run Anzor on the target model using only N trials.
- (2) Give the best schedule found with N trials to Droplet Search.
- (3) Run Droplet Search up to convergence.

Figure 8 provides some intuition on this *modus operandi*. As the figure illustrates, the proposed technique seeks to use Anzor to explore the universe of sketches and then use Droplet Search as the core strategy to explore concrete representations of these sketches.

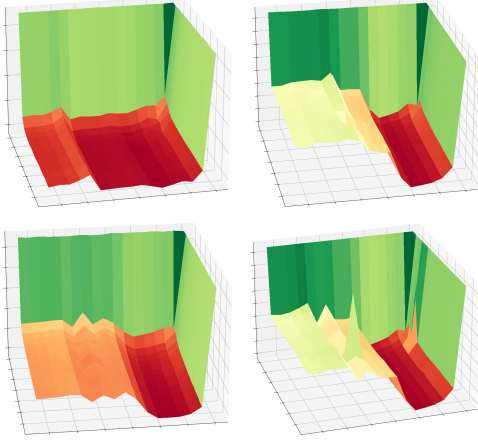
In Section 3, we demonstrate that by choosing proper values for K and N , we can outperform Anzor in two ways: first, producing faster end-to-end machine learning models; second, reducing the search time of Anzor. The modifications needed to add this combination to the current code base of Apache TVM are relatively small: up to 307 lines of code in the TVM repository (Release 17, Apache TVM v0.15.0).

3 EVALUATION

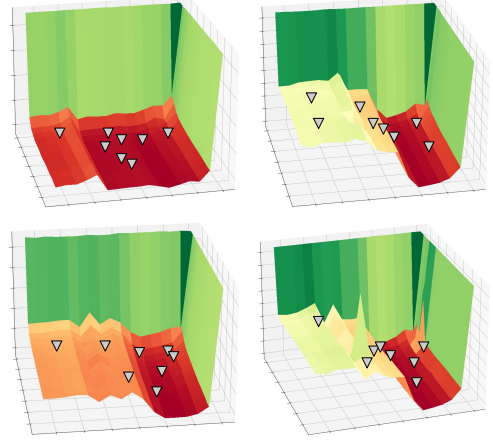
This section evaluates the idea proposed in this paper. In particular, it seeks to demonstrate that by exploiting, via Droplet Search, a reduced set of samples explored by Anzor, it is possible to outperform Anzor itself. We shall refer to this new version of Anzor, which uses Droplet Search, as the *Combined Approach*. Henceforth, we denote it as DPAnzor, reserving Anzor for the original implementation of that tool. In what follows, we explore six research questions:

- RQ1:** How many samples does DPAnzor need to observe to produce kernels that outperform those produced by Anzor with 10,000 trials?
- RQ2:** How many samples can DPAnzor observe and still outperform Anzor in terms of search time when the latter uses 10,000 trials?
- RQ3:** How does the size of models impact the behavior of DPAnzor, in terms of kernel performance and search speed?
- RQ4:** How does Droplet Search compare to other search techniques available in AutoTVM, in terms of their ability to exploit Anzor’s results?
- RQ5:** How does the average number of samples that Droplet Search gauges per layer vary with the initial budget allocated to DPAnzor’s exploration phase?

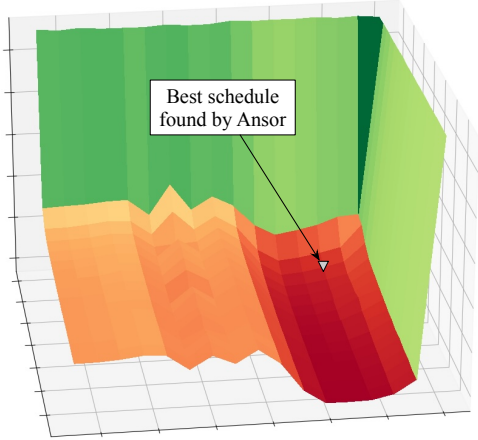
(a) Anso uses rewriting rules (Fig. 3) to produce different sketches. Each sketch determines a new kernel search space via the optimizations that it encodes.



(b) Anso annotates the sketches via initialization (Fig. 5) and evolution operations (Fig. 6). It runs some of the annotated sketches, to collect good kernel candidates.



(c) We choose the best schedule (annotated sketch), considering the running time of the end-to-end model.



(d) We give the best schedule to Droplet Search, which uses coordinate descent to explore its neighborhood.

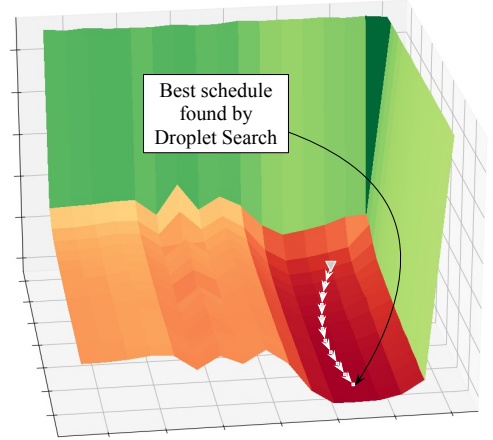


Fig. 8. Coarse exploration of different kernel search spaces with Anso, and careful exploitation of best candidate with Droplet Search.

RQ6: How does DPAnso compare with PyTorch and Anso in terms of the speed of the kernels that it produces, considering a range of different machine-learning kernels?

Before diving into the research questions, we explain our experimental setup. Notice that a fully containerized version of this methodology has been organized as a docker image, which is publicly available at <https://github.com/lac-dcc/bennu>.

Hardware and Software. We evaluated the scheduling approaches on four different architectures, as shown in Figure 9. The hardware consists of a general-purpose desktop architecture (AMD Ryzen 7 [AMD 2019]), a cluster-based machine (ARM A64FX [Ookami 2022]), and two graphics processing units (NVIDIA A100 [Nvidia 2020a] and NVIDIA RTX3080 [Nvidia 2020b]). The experiments reported in this section use versions of Anso and AutoTVM (Droplet Search) available at Apache

TVM v0.13.0, released in July 2023. The version used for TensorFlow was 2.14, and PyTorch was 2.0+cu118.

Device	Architecture	ISA	Clock Max (GHz)	Memory			
				RAM (GB)	Cache L1 (MiB)	Cache L2 (MiB)	Cache L3 (MiB)
AMD R7-3700X	x86-64	x86-64 (x86)	4.4	64	0.512	4	32
ARM A64FX	aarch64	ARMv8.2 + SVE	2.2	32	6	32	-
Nvidia A100	Ampere	PTX	1.4	40	-	-	-
Nvidia RTX3080	Ampere	PTX	1.7	12	-	-	-

Fig. 9. The architectures evaluated in this report.

Benchmarks. This section evaluates kernel scheduling across twenty neural networks. The first column of Figure 10 contains the complete list of these models. All these models are implemented using the ONNX representation to make a comparison between TVM, PyTorch and TensorFlow possible, as seen in Section 3.6. The models used in our study are sourced from the ONNX model zoo available at <https://github.com/onnx/models>.

Methodology. A machine learning model forms a graph of *kernels*. Ansoir optimizes machine learning models per kernel, assuming kernels can be independently optimized. It starts with a *budget of trials*, where each trial is a transformation that can be applied to a kernel. Let us call this budget K . Ansoir ensures that each kernel receives a fraction of these K trials. Currently, this initial fraction is $\min(K/L, 64)$, where L is the number of layers (kernels) in the model. After an initial round of optimizations, Ansoir applies the remaining trials onto kernels that run for the longest time. This approach directs the optimization effort to the kernels that are more likely to contribute to the overall running time of the end-to-end model. In what follows, all the results we report are relative to a baseline version of Ansoir equipped with a budget of 10,000 trials. We shall test DPAnsoir with either $K = 1, 10, 25, 50, 100, 200, 300$, or 1,000 trials. Suppose we choose $K = 100$, for instance. In that case, we will run Ansoir with a budget of 100 trials, pick the best configuration (which results from the independent optimization of the kernels), and give this configuration to AutoTVM’s Droplet Search. We then let Droplet Search run until it reaches convergence.

Confidence. Sections 3.1-3.4 show relative results. It could be possible that the running times presented for kernels and schedulers is similar enough to the point of hindering our conclusions meaningless. However, such is not the case. Scheduling runs for a very long time. To give the reader an idea, Ansoir, with a budget of 10,000 trials (or baseline), takes 11,195 seconds to schedule AlexNet, our smallest model. This time drops to 2,839 seconds considering DPAnsoir with a budget of 300 trials. The running time of kernels is faster: end-to-end models run for a few seconds. However, in every experiment, we consider averages of three samples and only report speedups if the p-value (produced via the non-parametric Wilcoxon rank-sum test) for the difference between the two populations is below 0.01.

3.1 RQ1 – On the Quality of End-to-End Models

We consider that a version of an end-to-end model is better than another for a given architecture when it runs faster in that architecture. The execution time of a model is determined by the schedule of the kernels that constitute it. If we apply Droplet Search to the best model produced by Ansoir after it observes 10,000 trials, we will likely improve the model (at least, we should not make it worse). However, this section shows that obtaining a better model via DPAnsoir with a much lower budget is possible in four different architectures. For brevity, we analyze in details results obtained on an x86 CPU. For the other architectures, we show only summarization results.

Discussion: AMD Ryzen 7 (x86-64). The x86 architecture represents a widely adopted instruction set architecture (ISA), serving as the basis for Intel and AMD processors. Figure 10 compares kernel speed and search time of models running on an x86-64 CPU. The top part of the figure (labeled “10k speedup execution time”) compares the running time of the kernels produced by Ansoor and DPAnsoor. The lower part (labeled “10k speedup tuning time”) compares the search time of these two approaches, and shall be discussed in Section 3.2. In both cases, bars above 1.0 denote improvements of DPAnsoor over Ansoor. In terms of kernel speed, sampling 25 configurations with DPAnsoor is sufficient—in most models—to outperform Ansoor with 10K samples. Speedups improve gradually as more samples are added to DPAnsoor, to the point that with 1,000 samples, we see an average speedup (geometric mean) of 34%.

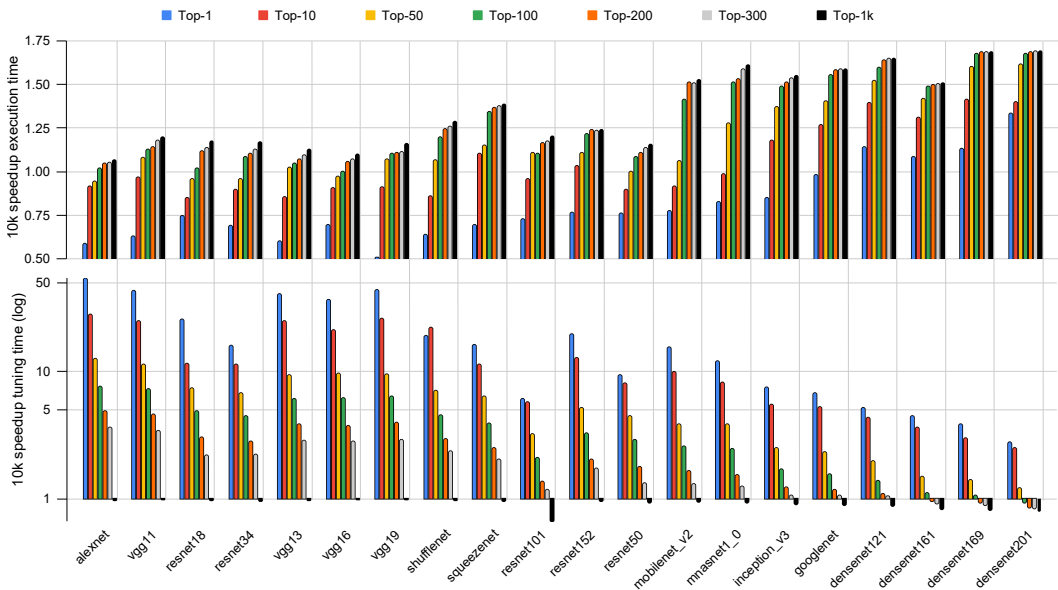


Fig. 10. Comparative Analysis of Optimization Results on the x86 Architecture Using an AMD Ryzen 7 3700X Processor. Numbers show Ansoor/DPAnsoor ratios. Thus, results higher than 1.0 (in blue) denote improvements of DPAnsoor (this paper) over Ansoor.

Discussion: Other Architectures. Figure 11 (Left) compares the relative speed of kernels produced by DPAnsoor over Ansoor in all the four architectures available for this study: in addition to the AMD x86 of Figure 10, we see an Nvidia A100(Ampere), an Nvidia RTX3080 (Ampere), and an ARM A64FX (aarch64). In every case, speedups of DPAnsoor relative to Ansoor emerge consistently with $K = 300$. However, with $K = 100$, we have already recorded speedups on the Nvidia A100 and on the ARM A64. We failed to see meaningful speedups on the Nvidia RTX3080 because Ansoor, with a budget of 10K samples, seems to be very close to achieving peak performance on this GPU. Even if we increase its budget of samples, we could not obtain better kernels to the 20 different models used in this study. Nevertheless, notice that DPAnsoor achieves this peak performance with 300 samples (plus a few—less than 50—samples probed by Droplet Search). On the A100 GPU, in contrast, after 300 samples, DPAnsoor already delivers kernels 12% faster than those produced by Ansoor.

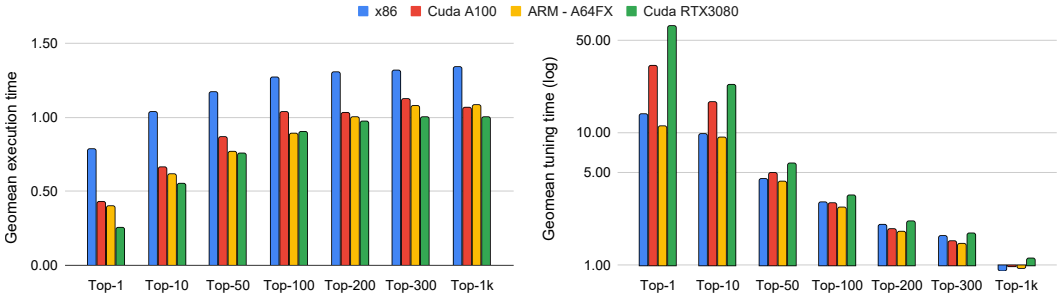


Fig. 11. Left: relative speed of kernels produced by DPAnsoor over Ansoor on four different architectures. Right: relative search time of DPAnsoor over Ansoor. Every bar is the geometric mean of relative times observed on 20 different models. Results above 1.0 represent improvements of DPAnsoor over Ansoor.

3.2 RQ2 – On the Search Time

We define a scheduling approach as faster than another if it requires less time to converge to an end-to-end model’s final, optimized version. The search time of Ansoor encompasses the time spent applying optimizations to kernels, deriving new optimizations, and running the kernels themselves, with a limit set at 10,000 trials. On the other hand, the search time of DPAnsoor involves all the steps of Ansoor, constrained to a lower number of trials, along with the time it takes to run Droplet Search until convergence on the kernels that compose a model. Although we have restricted Droplet Search to a maximum of 100 trials, it typically converges well before reaching that limit. This section compares the search time between Ansoor and DPAnsoor.

Discussion. The lower part of Figure 10 compares search times on x86. For most models, DPAnsoor is consistently faster than Ansoor for any number of trials up to $K = 300$. At 1,000 trials, Ansoor becomes consistently faster. Also, Ansoor tends to outperform DPAnsoor for very large models. This fact happens due to the longer time that Droplet Search takes to converge: the more complex the model, the more room Droplet Search will have to optimize it. Section 3.3 further discusses the impact of the model size on the behavior of DPAnsoor. Figure 11 summarizes the search time comparison for the other architectures. The pattern is similar to the one observed on x86: DPAnsoor is consistently faster when $K \leq 300$, and slower (except on the Nvidia RTX3080) at $K = 1,000$.

3.3 RQ3 – On the Impact of Model Size

The behavior of DPAnsoor, when compared to Ansoor, varies with the model’s size. We summarize this variation with two observations:

- (1) The larger the model, the less samples DPAnsoor needs to observe to outperform Ansoor, if Ansoor uses a budget of 10,000 samples.
- (2) The larger the model, the lower the benefit, in terms of search time, of DPAnsoor over Ansoor.

The rest of this section provides data to support these two conclusions.

Discussion: The Search vs Quality Slope. The kernel optimization technique impacts two core numbers: the search time and the speed of the final model. We can use these two quantities—search time (S) and model performance (P)—to define an $S \times P$ line characterizing the behavior of the optimization technique. Figure 12 shows these lines regarding four models and two architectures: AMD’s x86 and NVIDIA’s Ampere. We chose these two architectures because x86 is the scenario where DPAnsoor performs better, and Ampere is the scenario where it performs worse.

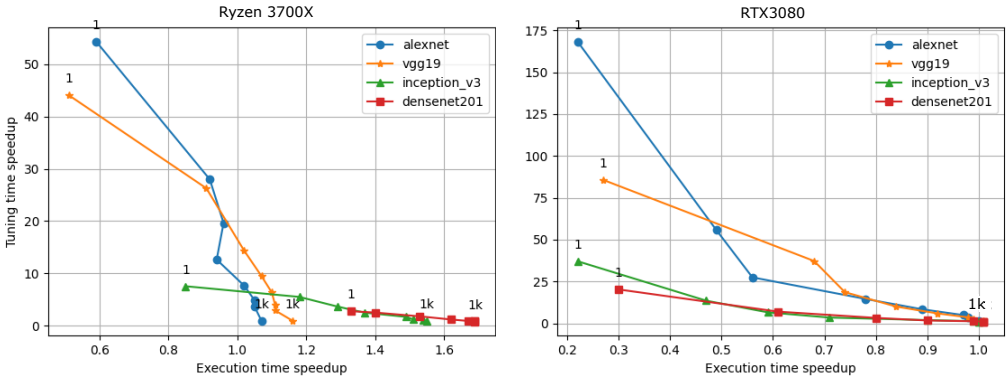


Fig. 12. The search vs quality line that characterizes four models optimized in the AMD (Left) and in the NVIDIA (Right) setting: the larger the model, the lower the slope. Numbers on the X and Y axes are speedup/slowdown relative to Ansor with a budget of 10,000 trials. Numbers for the left chart are available in Figure 10, and numbers for the right chart were observed on the Nvidia RTX3080. The labels on the dots (1 and 1k) refer to the number of trials given to DPAnso.

Figure 12 uses our two smallest and two largest models. The numbers on the axes show ratios between DPAnso and Ansor; the latter using a budget of 10,000 trials. Each dot in Figure 12 refers to the number of trials that DPAnso is allowed to observe before shifting to Droplet Search. The figure labels dots that refer to DPAnso with one sample (its most restrictive scenario) and dots that refer to 1,000 samples (its least restrictive scenario).

The slopes of the lines in Figure 12 are always negative, meaning that as more samples are given to DPAnso, the difference between its search time and Ansor’s reduces, but the quality of the kernels that it finds improves. However, the inclination changes with the size of the model. The larger the model, the lower the benefit of DPAnso over Ansor in terms of search time; but the higher the relative benefit in terms of kernel speed. This result is due to Ansor’s fixed budget of 10,000 trials. In a small model, more trials are distributed to each layer; in a large model, each layer receives only a handful of trials.

Figure 13 provides further data that supports the previous observations. The figure shows how kernel quality and search time vary with the size of models. If we consider AlexNet, which has only 13 layers, each layer might receive, on average, $10^4/13$ trials. Inevitably, good kernels will emerge from this search. Thus, the benefit of the exploitation phase, which uses Droplet Search, tends to be smaller. On the other hand, if we consider DenseNet201, which has 113 layers, then Ansor allocates, on average, $10^4/113$ trials per layer—less than 100 samples per each kernel of the computational graph. This number is too low to effectively explore the space of possible kernel implementations. In this case, Droplet Search has more opportunity to improve the kernels that Ansor finds. Even using only one trial to find the origin of the optimization space is already enough to have DPAnso outperforming Ansor in terms of the quality of the model.

3.4 RQ4 – On the Search Technique

The core idea of this paper consists in using Droplet Search to exploit results produced by Ansor. Therefore, an immediate question from this proposal is: *what if other search techniques are used instead of Droplet Search, as the basic exploitation technique?* Indeed, AutoTVM, the framework hosting Droplet Search, provides four other search techniques that could fill the same role as Droplet Search. These techniques are described as follows:

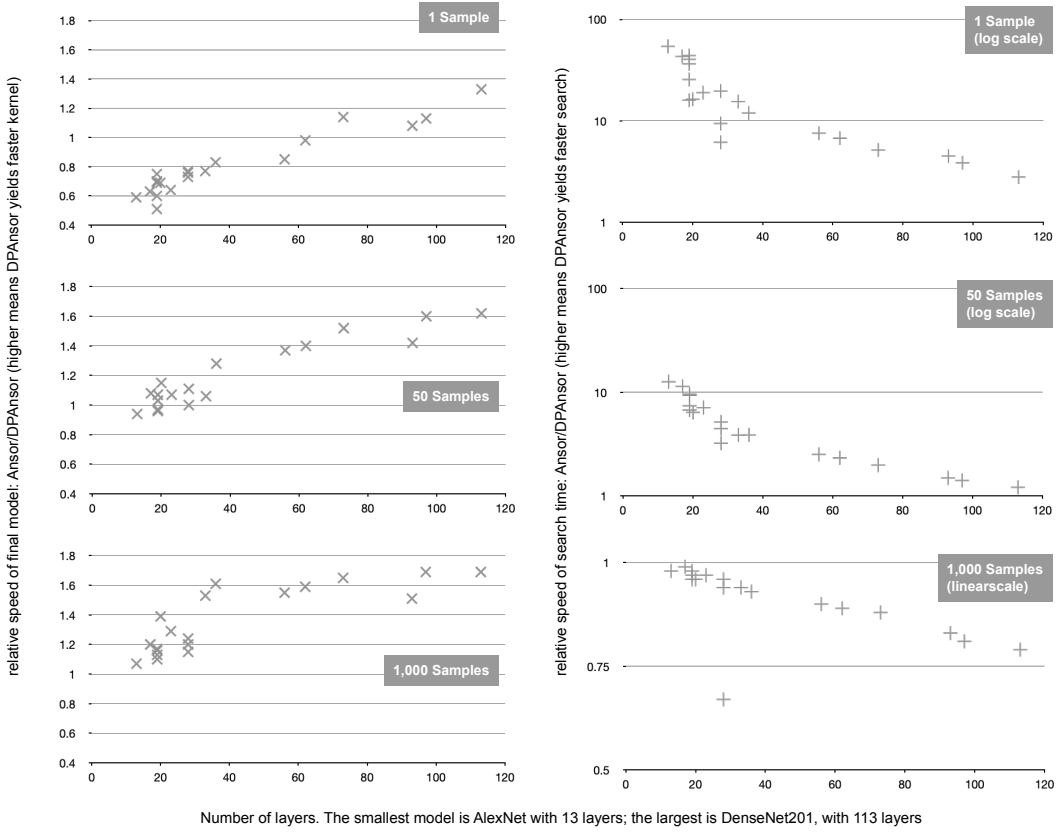


Fig. 13. (Left) Variation in kernel quality (Ansol/DPAnsol) with model size. (Right) Variation in search time (Ansol/DPAnsol) with model size.

Random: a random search on the space of valid optimization parameters. In this case, each sample is randomly produced. Search is stateless, meaning that the results of a kernel bear no influence on the choice of the next kernel.

Grid: a grid search on the space of valid parameters of the optimizations. In this case, each sample derives from a regular and exhaustive variation of each optimization parameter. Search keeps a minimum of state, namely, a counter per optimization parameter, that goes over the range of acceptable values.

GA: a genetic algorithm that treats the sequence of optimization parameters as chromosomes. Search is stateful: the running times of already seen kernels provide information to guide the synthesis of the next kernels via operations such as mutation, crossover and pruning.

XGB: search is based on gradient boosting, as implemented by the XGBoost Library [Chen and Guestrin 2016]. Similar to the genetic algorithm, the search is stateful, as the running time of kernels guides the construction of the search tree.

In the rest of this section, we analyze the behavior of DPAnsol, once its search technique (the “DP” part of Ansol) is replaced by each one of the other four algorithms available in AutoVM.

Methodology. Every experiment in this Section allocates a budget of 300 samples to Ansol for each model that we autotune. Exploitation, via one of the different search techniques in AutoVM,

uses a budget of 100 trials to optimize each layer of AlexNet. Droplet Search converged before 100 trials in every layer, but all the other approaches run 100 samples, as they do not have a notion of convergence. Thus, each other approach samples 1,200 kernel configurations. Each search technique in AutoTVM exploits the best sequence of optimizations found by Ansoor, which is the same for all of them. Following the methodology adopted in Section 3.3, we report results for the AMD x86 and the NVIDIA 3080 boards. These are the best and worst scenarios observed for DPAnsoor in Sections 3.1 and 3.2.

Discussion: AMD Ryzen 7 (x86-64). Figure 14 compares Droplet Search against other AutoTVM methods on the x86 architecture. As an exploitation technique, Droplet Search demonstrates superior performance in terms of execution time and kernel speedup. The **random** search technique is completely oblivious to the seed best provided by Ansoor. The **grid** search is almost oblivious to it: although the grid search starts from a likely good kernel, it diverges quickly from that configuration. The other techniques can benefit from Ansoor’s exploration phase. We feed both **GA** and **XGB** with a promising seed; however, these search techniques still need random seeds to diversify the initial population of kernels from where they depart. Because the other search techniques lack a convergence criterion, the relative performance of Droplet Search—in turning time—is even better: it is approximately 3x faster.

x86		Execution speedup				Tuning speedup			
Model	L	grid / droplet	random / droplet	ga / droplet	xgb / droplet	grid / droplet	random / droplet	ga / droplet	xgb / droplet
alexnet	13	3.04	2.55	2.27	2.04	3.55	5.05	3.62	3.93
vgg11	17	6.97	2.42	1.69	1.82	4.80	3.53	3.61	3.53
resnet18	19	8.28	2.22	1.97	2.40	2.29	2.81	3.05	3.09
resnet34	19	9.63	2.34	2.00	2.05	1.97	2.77	2.61	2.85
vgg13	19	6.51	3.15	2.27	2.19	4.86	4.37	4.26	3.72
vgg16	19	6.90	2.29	1.98	2.47	4.62	4.17	3.78	3.62
vgg19	19	6.60	2.20	1.93	2.32	4.46	3.71	4.18	3.76
shufflenet	20	2.30	2.41	2.34	2.23	4.78	7.50	6.74	7.21
squeezenet	23	2.40	3.31	2.52	2.25	3.24	4.89	4.65	4.58
resnet101	28	7.02	2.69	3.62	3.34	2.01	2.95	2.87	2.65
resnet152	28	6.87	2.21	2.63	2.09	2.40	3.10	3.08	3.11
resnet50	28	7.43	2.09	2.38	2.39	2.34	3.16	3.52	3.65
mobilenet_v2	33	3.27	2.67	3.19	2.69	3.61	5.60	5.67	5.47
mnasnet1_0	36	3.09	2.57	3.31	2.55	3.41	5.43	5.81	5.54
inception_v3	56	2.49	2.24	2.64	2.41	2.54	4.18	4.13	3.96
googlenet	62	2.71	2.12	2.29	2.33	2.61	4.05	3.77	3.88
densenet121	73	2.50	1.90	1.87	2.23	2.16	3.18	3.28	3.11
densenet161	93	2.65	2.30	2.49	2.47	2.06	3.39	3.18	3.24
densenet169	97	2.66	1.92	2.30	2.30	1.91	2.87	2.99	2.90
densenet201	113	2.58	2.07	2.54	2.52	1.84	2.82	2.76	2.77
GEO	-	4.21	2.36	2.37	2.34	2.90	3.82	3.75	3.70

Fig. 14. Comparison of different exploitation techniques used in tandem with Ansoor on the x86-64 setting. Numbers are ratio of “*SearchTechnique/DropletSearch*”. Thus, numbers above 1.0 demonstrate the effectiveness of the technique proposed in this paper.

Discussion: CUDA RTX 3080 (Ampere). In the GPU setting, Droplet Search is still a superior exploitation technique in terms of search time and kernel speed, as Figure 15 demonstrates. In contrast to the CPU setting, invalid kernels are common in the GPU scenario. AutoTVM does not

provide any way to constrain the search technique to using parameters that yield correct kernels. We observe, for instance, that the **Grid** search often generates invalid kernels, as the number of threads on the X, Y, and Z dimensions exceeds the total number of threads in the stream multiprocessor.

RTX 3080		Execution speedup				Tuning speedup			
Model	L	grid / droplet	random / droplet	ga / droplet	xgb / droplet	grid / droplet	random / droplet	ga / droplet	xgb / droplet
alexnet	13	6.10	2.74	1.28	1.22	2.85	5.43	3.14	3.63
vgg11	17	6.92	1.50	1.56	1.50	3.03	3.89	3.98	3.88
resnet18	19	15.74	3.35	2.06	2.12	1.75	2.36	2.45	2.53
resnet34	19	18.91	2.99	2.56	2.08	1.58	2.26	2.24	2.30
vgg13	19	9.98	1.89	2.12	1.82	2.68	5.15	5.05	4.17
vgg16	19	9.12	2.47	1.90	1.49	2.82	5.52	5.36	5.60
vgg19	19	10.25	2.84	4.09	1.58	3.25	4.91	5.09	5.47
shufflenet	20	4.38	3.62	2.42	2.37	2.96	3.94	3.82	3.88
squeezenet	23	9.36	3.53	3.28	2.44	2.64	3.24	3.16	3.47
resnet101	28	22.06	5.27	3.13	2.35	1.80	2.53	2.46	2.63
resnet152	28	21.36	4.90	3.95	2.66	2.10	2.80	2.99	3.08
resnet50	28	23.91	3.06	2.57	2.50	2.01	2.91	3.19	3.34
mobilenet_v2	33	8.99	3.21	2.56	2.66	2.14	2.82	2.64	2.70
mnasnet1_0	36	8.73	2.97	2.79	2.40	2.28	3.09	3.26	3.12
inception_v3	56	11.59	2.89	2.35	2.22	2.44	3.16	3.23	3.16
googlenet	62	10.44	3.22	2.54	2.32	1.97	2.63	2.56	2.65
densenet121	73	14.22	2.78	2.23	2.42	2.08	2.29	2.43	2.31
densenet161	93	12.60	3.95	3.14	2.21	2.01	2.13	2.00	2.04
densenet169	97	12.54	3.52	2.40	1.99	1.91	2.14	2.23	2.16
densenet201	113	12.31	3.48	2.49	2.17	1.84	2.12	2.08	2.10
GEO	-	11.42	3.10	2.48	2.08	2.26	3.10	3.03	3.08

Fig. 15. Comparison of different exploitation techniques used in tandem with Anzor on the Cuda setting. Numbers are ratio of “*SearchTechnique/DropletSearch*”. Thus, numbers above 1.0 demonstrate the effectiveness of the technique proposed in this paper.

Discussion: Universality of these Results. Droplet Search is not universally superior to the other search techniques available in AutoTVM, when used as an exploitation method in Anzor. For instance, if we analyze the behavior of these different search approaches per layer of AlexNet, we observe situations where Droplet Search yields slower kernels than the other methods. Figure 16 demonstrates this point. These subpar results happen due to the stochastic nature of all these autotuning techniques. Droplet Search might stop on a suboptimal kernel because its convergence criterion is statistical in nature: if the running time of kernels is considered similar with a confidence level of 95%, then the coordinate descent procedure stops. However, regarding search speed, we have not identified one single layer of AlexNet where Droplet Search would be slower than the other search approaches. Additionally, if we repeat the same analysis per layer of AlexNet on the GPU setting, we observe that Droplet Search is superior to the other search approaches in every layer. We omit these results from this paper for the sake of space.

3.5 RQ5: The Average Number of Droplet Search Samples

As hinted in Section 3.4, Droplet Search has a convergence criterion discussed in Section 3.3 of its description [Canesche et al. 2024]. In this case, the search stops once there is no statistically significant difference between the current kernel and the kernels within its neighborhood. Thus, the

x86 layer	Execution speedup				Tuning speedup			
	grid / droplet	random / droplet	ga / droplet	xgb / droplet	grid / droplet	random / droplet	ga / droplet	xgb / droplet
0	5.16	7.99	10.19	5.16	2.25	8.11	3.43	4.06
1	1.27	1.26	1.31	1.27	10.74	10.77	3.29	3.28
2	4.38	5.71	3.07	3.07	2.24	3.42	5.54	5.73
3	6.06	10.79	4.78	4.97	2.43	2.56	2.34	2.31
4	1.16	1.15	1.10	1.03	3.66	3.70	3.60	3.64
5	4.65	3.70	1.58	1.58	2.44	4.55	4.70	4.24
6	0.99	0.98	0.95	0.95	10.68	13.37	3.25	3.32
7	5.57	5.32	5.70	5.32	2.77	3.25	3.11	3.49
8	4.28	1.96	3.12	1.96	2.31	4.07	4.40	4.12
9	0.99	0.99	1.08	0.99	3.97	3.99	2.08	2.08
10	3.30	0.74	0.70	0.70	7.10	8.44	7.02	8.41
11	4.32	1.66	1.55	1.55	2.54	8.69	4.20	8.43
12	6.10	5.90	6.20	6.01	2.47	2.09	2.74	2.80
GEO	3.04	2.55	2.27	2.04	3.55	5.05	3.62	3.93

Fig. 16. Results of Figure 14, analyzed per layer of AlexNet.

more optimized the seed of the coordinate descent algorithm, the fewer iterations it is intuitively expected to take until convergence. This section investigates if this hypothesis is true.

Discussion. We count the number of iterations of Droplet Search on our different architectures, considering different budgets for DPAnzor. Figure 17 shows this number for each model evaluated on the x86 setting. The figure reports a total number of trials and an average number of trials per layer. The general tendency is that the larger the budget of trials allocated to DPAnzor, the faster Droplet Search converges.

Figure 18 summarizes, for each architecture, the numbers earlier seen in Figure 17. Figure 18 reports averages per model (considering the 20 available models), and averages per layer. In the latter case, we divide the total sum of trials observed for all the models by the sum of the number of layers present in every model. In every case, the same tendency is evident: more trials sampled during exploration imply fewer trials sampled during exploitation. This result is intuitive: as previously mentioned, Droplet Search tends to reach stability the closer to a local optimum it starts.

3.6 RQ6: Comparison with Well-Known Machine-Learning Frameworks

Thus far, the results we evaluated in this section are constrained to the Apache TVM software stack. To provide the reader with some perspective on these results, we shall compare Anzor and DPAnzor with two well-known deep-learning frameworks: PyTorch 2.0 [Paszke et al. 2019] and TensorFlow v2.15.0 [Singh et al. 2020]. Recently, Ansel et al. [2024] have shown that PyTorch is able to outperform Anzor in many different workloads. However, in Ansel et al.’s setting, Anzor was used as a backend, without autotuning the target kernels. In this section we activate autotuning for Anzor and DPAnzor. To this end, we give Anzor a budget of 1,000 trials. In contrast, we use DPAnzor, either with a budget of 100 or 300 trials before activating Droplet Search.

Discussion. Figure 19 summarizes the results of the comparison of different deep-learning tools. In our setting, PyTorch is consistently faster than TensorFlow on the two different graphics processing units available for these experiments. However, Anzor and DPAnzor outperform PyTorch on large workloads (matmul, conv2d, depthwise and pooling). Corroborating these results, the benefit of Anzor over PyTorch was also observed by Li et al. [2021]. Notice that these results do not include two kernels, reduce and ReLU. In these two cases, neither Anzor nor DPAnzor have much room to

x86-64		Sum of trials							Average trials per layer						
Model	L	Top-1 Anzor	Top-10 Anzor	Top-50 Anzor	Top-100 Anzor	Top-200 Anzor	Top-300 Anzor	Top-1k Anzor	Top-1 Anzor	Top-10 Anzor	Top-50 Anzor	Top-100 Anzor	Top-200 Anzor	Top-300 Anzor	Top-1k Anzor
alexnet	13	187	201	205	199	169	162	171	14	15	16	15	13	12	13
vgg11	17	232	210	185	172	158	158	160	14	12	11	10	9	9	9
resnet18	19	428	437	441	351	316	328	318	23	23	23	18	17	17	17
resnet34	19	427	419	359	387	428	350	351	22	22	19	20	23	18	18
vgg13	19	245	274	245	213	190	177	187	13	14	13	11	10	9	10
vgg16	19	263	228	230	193	218	185	186	14	12	12	10	11	10	10
vgg19	19	216	240	215	233	207	189	204	11	13	11	12	11	10	11
shufflenet	20	295	297	256	287	271	275	272	15	15	13	14	14	14	14
squeezenet	23	489	557	390	421	381	370	364	21	24	17	18	17	16	16
resnet101	28	818	860	759	694	674	684	655	29	31	27	25	24	24	23
resnet152	28	841	726	784	699	687	704	720	30	26	28	25	25	25	26
resnet50	28	925	839	784	757	643	657	644	33	30	28	27	23	23	23
mobilenet_v2	33	524	532	606	603	486	539	524	16	16	18	18	15	16	16
mnasnet1_0	36	706	678	696	706	653	678	685	20	19	19	20	18	19	19
inception_v3	56	1410	1393	1344	1239	1272	1263	1270	25	25	24	22	23	23	23
googlenet	62	1430	1384	1350	1333	1335	1311	1310	23	22	22	22	22	21	21
densenet121	73	2070	1823	1768	1648	1756	1696	1736	28	25	24	23	24	23	24
densenet161	93	2530	2381	2359	2269	2282	2271	2280	27	26	25	24	25	24	25
densenet169	97	2665	2513	2419	2435	2387	2485	2484	27	26	25	25	25	26	26
densenet201	113	3110	3004	2846	2955	3063	2890	2946	28	27	25	26	27	26	26
AVG	-	991	950	912	890	879	869	873	22	21	20	19	19	18	18

Fig. 17. Number of trials sampled by Droplet Search until reaching convergence, considering the AMD x86-64 architecture. The average number of trials per layer divides the total number of trials per the number of layers in each deep learning model.

Arch	Sum of trials							Average trials per layer						
	Top-1 Anzor	Top-10 Anzor	Top-50 Anzor	Top-100 Anzor	Top-200 Anzor	Top-300 Anzor	Top-1k Anzor	Top-1 Anzor	Top-10 Anzor	Top-50 Anzor	Top-100 Anzor	Top-200 Anzor	Top-300 Anzor	Top-1k Anzor
x86-64	19811	18996	18241	17794	17576	17372	17467	24	23	22	22	22	21	21
ARM A64FX	19610	17785	15768	14450	13506	13683	13072	24	22	19	18	17	17	16
Cuda RTX3080	17803	13982	11886	10965	10779	10751	10819	22	17	15	13	13	13	13
Cuda A100	24831	20278	17147	14655	13731	14110	13832	30	25	21	18	17	17	17

Fig. 18. Average number of trials per model (considering 20 models) for different architectures. The averages per layer are the quotient of the total number of trials for all the models divided by the total number of layers.

perform optimizations. These kernels show minimal memory reuse: they visit each memory cell only once, and little benefit can be acquired from autotuning. As a consequence, the search time is very short when compared with the search time spent on the larger kernels.

4 RELATED WORK

The design and implementation of systems to run machine learning models have been experiencing constant progress. Following [Ding et al. \[2023\]](#), we recognize two main approaches to run deep-learning models, which we call *interpretation* and *compilation*. In the former approach, frameworks such as PyTorch [[Paszke et al. 2019](#)], TensorFlow [[Abadi et al. 2016](#)], and the ONNX runtime [[Jin et al. 2020](#)] implement machine learning models by binding operations to libraries such as cuDNN, cuBLAS, and CUTLASS. In the latter approach, tools such as TVM, Halide [[Ragan-Kelley et al. 2013](#)], TorchInductor [[Ansel et al. 2024](#)] or XLA generate code for the operations that constitute the model. This work concerns compilation; nevertheless, to provide some perspective to the reader about the relative effectiveness of these systems, Section 3.6 compares our approach with standard

RTX 3080	Tensorflow	Pytorch	Anso ^r (1000 samples)		DPA ⁿ so ^r (100 samples)		DPA ⁿ so ^r (300 samples)	
Microkernel	exec time (ms)	exec time (ms)	exec time (ms)	tuning time (min)	exec time (ms)	tuning time (min)	exec time (ms)	tuning time (min)
matmul	0.49759126	0.123663	0.012660	37.96	0.0112784	3.60	0.0081228	8.02
conv2d	10.43869758	2.146128	1.819560	72.39	2.0869700	8.19	1.7976000	19.76
depthwise	4.06337643	3.824702	0.650381	64.67	0.6952420	10.72	0.6530620	21.67
pooling	1.34876990	0.957267	0.974534	71.90	0.9545340	8.66	0.9545340	21.91
reduce	1.31569195	0.314016	0.312430	2.69	0.3124030	2.70	0.3124030	2.72
relu	1.21619201	0.165822	0.172650	0.18	0.1721830	0.19	0.1721830	0.19
A100	Tensorflow	Pytorch	Anso ^r (1000 samples)		DPA ⁿ so ^r (100 samples)		DPA ⁿ so ^r (300 samples)	
matmul	0.1473048	0.032737	0.013206	41.88	0.0144076	6.3	0.0103285	11.4
conv2d	8.6722476	2.401592	2.025246	73.21	2.2853300	12.09	2.0056600	25.3
depthwise	3.7513964	2.881968	0.422472	93.08	0.6085967	15.75	0.4215467	29.59
pooling	3.1504140	0.935589	0.881824	84.95	0.9825180	9.1	0.8918100	25.33
reduce	1.7370601	0.192991	0.157589	3.92	0.1562760	2.9	0.1562760	2.9
relu	1.0123856	0.119100	0.172235	0.46	0.1972600	0.25	0.1972600	0.25

Fig. 19. Comparison between the running time of kernels produced via TensorFlow, PyTorch, Anso^r or DPAⁿso^r running on two different GPUs. The black cells highlight fastest results; the gray cells indicate ties (with confidence level of 95%). TensorFlow and PyTorch do not perform tuning.

distributions of PyTorch and TensorFlow. Contrary to the findings in Section 3.6, Ansel et al. have recently shown that PyTorch, in compilation mode, consistently outperforms Anso^r. However, in those experiments, Anso^r was used solely as a code generator without performing any autotuning. In our setup, once autotuning is enabled, Anso^r can outperform PyTorch in most kernels.

Design and Construction of Autotuners. The original presentations of AutoTVM [Chen et al. 2018] and Anso^r [Zheng et al. 2020] outline the key techniques utilized in this paper. These tools explore optimizations typically described via the *polyhedral model* [Fautrier 1996]. Said optimizations, including fusion, tiling, and fission, are commonplace in tools such as POLLY [Grosser et al. 2012], GRAPHITE [Trifunovic et al. 2010] and PLuTo [Bondhugula et al. 2008]. These tools do not solve the autotuning problem; however, they offer the basic infrastructure to do so, as Tavarageri et al. [2021] have demonstrated with their POLYDL framework.

Recent research focuses on pruning the search space to enhance the efficiency of autotuners. For instance, Tollenaere et al. [2023]’s search algorithm uses a cost model to avoid exploring regions of the kernel space unlikely to yield good schedules. However, building an accurate analytical model seems an illusive problem. In the words of Ritter and Hack [2024]: “Modern processor designs use many techniques to improve overall performance that cause complex, irregular performance characteristics.” Additionally, there has been much work into adapting autotuners to deal with tensors whose shape is not statically known [Mururu et al. 2023; Pfaffe et al. 2019]. For instance, DIETCODE [Zheng et al. 2022] and SoD² [Niu et al. 2024] use a cost model similar to Tollenaere et al.’s, to represent the shape of a tensor as symbols that will only be known at runtime. We notice that autotuning is not restricted to scheduling the order of computations within a kernel. For instance, autotuning techniques can be used to choose the format to store tensors (sparse vs dense) [Ahrens et al. 2022; Dhandhanian et al. 2021; Won et al. 2023], or the bitwidth used for quantization [Hubara et al. 2021; Kloberdanz and Le 2023].

This paper does not propose a new kernel scheduling algorithm. Rather, it is bringing forward the observation that the combination of two well-established heuristics tend to bring much benefit to the generation of high-quality kernels. This benefit is measured not only in terms of the speed of

the final code, but also in terms of the efficiency of the search technique. In this sense, an important consequence of our work is the fact that it makes AnsoR more hardware-aware. By using coordinate descent as an exploitation approach, AnsoR’s search remains circumscribed to a region that is likely to benefit more from the available hardware. Some research groups have, independently, shown that the design of hardware-centric (in contrast to input-centric) autotuners tend to accelerate the search process [Ding et al. 2023; Li et al. 2024; Zhu et al. 2022]. This paper demonstrates this point without designing an algorithm that needs to be parameterized with hardware characteristics.

5 CONCLUSION

This paper has defended the thesis that state-of-the-art kernel scheduling methodologies can greatly benefit from a simple exploitation phase based on coordinate descent. To support this thesis, we have implemented a combined exploration/exploitation search methodology in AnsoR. The new approach uses AnsoR to explore different kernel optimization spaces and uses Droplet Search as a post-exploration phase. This methodology improves AnsoR and Droplet Search in different ways:

- It enhances AnsoR’s capability to exploit “hardware boundaries”. The previous implementation of AnsoR was not aware of the relationships between neighboring kernel schedules, as it lacked a concept of “distance” between the implementations of kernels. The new exploration phase improves AnsoR’s ability to better adjust optimization parameters to hardware constraints, such as cache sizes and vector widths.
- It addresses Droplet Search’s two limitations: its reliance on a well-defined *seed* (the initial kernel that initiates coordinate descent), and its inability to explore different kernel spaces. Previously, the seed and the kernel space were determined manually, requiring a programmer to provide Droplet Search with an initial annotated sketch [Canesche et al. 2024; Li et al. 2024]. The proposed methodology automates the seed generation process by utilizing AnsoR.

As Section 3 demonstrates, the proposed extension improves AnsoR in terms of kernel quality and search time. A container to reproduce those experiments is available at <https://github.com/lac-dcc/bennu>. That implementation has been submitted to the AnsoR community in late 2023 [Canesche 2023]. A similar extension was later deployed onto TVM’s MetaSchedule [Canesche 2024], achieving even better results than those seen in Section 3. Thus, we believe that this combination of a wide exploration phase and a fine-grained exploitation step implemented via coordinate descent is general enough to be incorporated into different kernel schedulers.

ACKNOWLEDGMENT

This project was sponsored by Cadence Design Systems. The authors extend their gratitude to Eric Stotzer and Vanderson Rosário for facilitating Cadence’s financial support. Additionally, the authors acknowledge the support of CNPq (grants 314645/2020-9 and 406377/2018-9), FAPEMIG (grant PPM-00333-18), and CAPES (Edital PRINT). The experiments in Section 3 were conducted using hardware generously provided by the Ookami Computing Center, through US NSF grant #192788, and by the Flatiron Institute, NY. The authors express their appreciation to the TVM Community for the discussions that helped shape this work.

REFERENCES

Martin Abadi, Paul Barham, Jianmin Chen, Zhifeng Chen, Andy Davis, Jeffrey Dean, Matthieu Devin, Sanjay Ghemawat, Geoffrey Irving, Michael Isard, Manjunath Kudlur, Josh Levenberg, Rajat Monga, Sherry Moore, Derek G. Murray, Benoit Steiner, Paul Tucker, Vijay Vasudevan, Pete Warden, Martin Wicke, Yuan Yu, and Xiaoqiang Zheng. 2016. TensorFlow: a system for large-scale machine learning. In *OSDI (Savannah, GA, USA) (OSDI’16)*. USENIX Association, USA, 265–283.

- Willow Ahrens, Fredrik Kjolstad, and Saman Amarasinghe. 2022. Autoscheduling for sparse tensor algebra with an asymptotic cost model. In *PLDI* (San Diego, CA, USA). Association for Computing Machinery, New York, NY, USA, 269–285. <https://doi.org/10.1145/3519939.3523442>
- AMD. 2019. AMD Ryzen™ 7 3700X. <https://www.amd.com/en/product/8446>. [Online; accessed 18-Jan-2024].
- Jason Ansel, Edward Yang, Horace He, Natalia Gimelshein, Animesh Jain, Michael Voznesensky, Bin Bao, Peter Bell, David Berard, Evgeni Burovski, Geeta Chauhan, Anjali Chourdia, Will Constable, Alban Desmaison, Zachary DeVito, Elias Ellison, Will Feng, Jiong Gong, Michael Gschwind, Brian Hirsh, Sherlock Huang, Kshiteej Kalambarkar, Laurent Kirsch, Michael Lazos, Mario Lezcano, Yanbo Liang, Jason Liang, Yinghai Lu, CK Luk, Bert Maher, Yunjie Pan, Christian Puhersch, Matthias Reso, Mark Saroufim, Marcos Yukio Siraichi, Helen Suk, Michael Suo, Phil Tillet, Eikan Wang, Xiaodong Wang, William Wen, Shunting Zhang, Xu Zhao, Keren Zhou, Richard Zou, Ajit Mathews, Gregory Chanan, Peng Wu, and Soumith Chintala. 2024. PyTorch 2: Faster Machine Learning Through Dynamic Python Bytecode Transformation and Graph Compilation. In *ASPLOS*. ACM, New York, USA, 623–630.
- Uday Bondhugula, Albert Hartono, J. Ramanujam, and P. Sadayappan. 2008. A practical automatic polyhedral parallelizer and locality optimizer. In *PLDI* (Tucson, AZ, USA) (*PLDI '08*). Association for Computing Machinery, New York, NY, USA, 101–113. <https://doi.org/10.1145/1375581.1375595>
- Michael Canesche. 2023. [RFC] Combine Ansoor and AutoTVM to Improve Scheduling. <https://discuss.tvm.apache.org/t/rfc-combine-ansoor-and-autotvm-to-improve-scheduling/16337>. Experimental results are listed on a report that is publicly available at https://homepages.dcc.ufmg.br/~michaelcanesche/paper/bennu_meta_version.pdf.
- Michael Canesche. 2024. [RFC] Adding an Exploitation Phase to MetaSchedule to Improve Scheduling. <https://discuss.tvm.apache.org/t/rfc-metaschedule-adding-an-exploitation-phase-to-metaschedule-to-improve-scheduling/17365>. Experimental results are listed on a report that is publicly available at https://homepages.dcc.ufmg.br/~michaelcanesche/paper/bennu_meta_version.pdf.
- Michael Canesche, Vanderson M. Rosario, Edson Borin, and Fernando Magno Quintão Pereira. 2024. The Droplet Search Algorithm for Kernel Scheduling. , 25 pages. <https://doi.org/10.1145/3650109> Just Accepted.
- Tianqi Chen and Carlos Guestrin. 2016. XGBoost: A Scalable Tree Boosting System. In *KDD* (San Francisco, California, USA). Association for Computing Machinery, New York, NY, USA, 785–794. <https://doi.org/10.1145/2939672.2939785>
- Tianqi Chen, Thierry Moreau, Ziheng Jiang, Lianmin Zheng, Eddie Yan, Haichen Shen, Meghan Cowan, Leyuan Wang, Yuwei Hu, Luis Ceze, et al. 2018. {TVM}: An automated {End-to-End} optimizing compiler for deep learning. In *OSDI/USENIX*, Berkeley, USA, 578–594.
- Sunidhi Dhandhania, Akshay Deodhar, Konstantin Pogorelov, Swarnendu Biswas, and Johannes Langguth. 2021. Explaining the Performance of Supervised and Semi-Supervised Methods for Automated Sparse Matrix Format Selection. In *ICPP* (Lemont, IL, USA). Association for Computing Machinery, New York, NY, USA, Article 6, 10 pages. <https://doi.org/10.1145/3458744.3474049>
- Yaoyao Ding, Cody Hao Yu, Bojian Zheng, Yizhi Liu, Yida Wang, and Gennady Pekhimenko. 2023. Hidet: Task-Mapping Programming Paradigm for Deep Learning Tensor Programs. In *ASPLOS* (Vancouver, BC, Canada). Association for Computing Machinery, New York, NY, USA, 370–384. <https://doi.org/10.1145/3575693.3575702>
- Paul Feautrier. 1996. Automatic Parallelization in the Polytope Model. In *The Data Parallel Programming Model: Foundations, HPF Realization, and Scientific Applications*. Springer-Verlag, Berlin, Heidelberg, 79–103.
- Tobias Grosser, Armin Größlinger, and Christian Lengauer. 2012. Polly - Performing Polyhedral Optimizations on a Low-Level Intermediate Representation. *Parallel Process. Lett.* 22, 4 (2012), 23 pages. <https://doi.org/10.1142/S0129626412500107>
- Itay Hubara, Yury Nahshan, Yair Hanani, Ron Banner, and Daniel Soudry. 2021. Accurate Post Training Quantization With Small Calibration Sets. In *Proceedings of the 38th International Conference on Machine Learning (Proceedings of Machine Learning Research, Vol. 139)*, Marina Meila and Tong Zhang (Eds.). PMLR, Maastricht, NL, 4466–4475.
- Tian Jin, Gheorghe-Teodor Bercea, Tung D. Le, Tong Chen, Gong Su, Haruki Imai, Yasushi Negishi, Anh Leu, Kevin O’Brien, Kiyokuni Kawachiya, and Alexandre E. Eichenberger. 2020. Compiling ONNX Neural Network Models Using MLIR. arXiv:2008.08272 [cs.PL]
- Eliska Kloberdanz and Wei Le. 2023. MixQuant: Mixed Precision Quantization with a Bit-width Optimization Search. arXiv:2309.17341 [cs.LG]
- Chendi Li, Yufan Xu, Sina Mahdipour Saravani, and Ponnuswamy Sadayappan. 2024. Accelerated Auto-Tuning of GPU Kernels for Tensor Computations. In *ICS* (Kyoto, Japan). Association for Computing Machinery, New York, NY, USA, 549–561. <https://doi.org/10.1145/3650200.3656626>
- Rui Li, Yufan Xu, Aravind Sukumaran-Rajam, Atanas Rountev, and P. Sadayappan. 2021. Analytical characterization and design space exploration for optimization of CNNs. In *ASPLOS* (Virtual, USA). Association for Computing Machinery, New York, NY, USA, 928–942. <https://doi.org/10.1145/3445814.3446759>
- Girish Mururu, Sharjeel Khan, Bodhisatwa Chatterjee, Chao Chen, Chris Porter, Ada Gavrilovska, and Santosh Pande. 2023. Beacons: An End-to-End Compiler Framework for Predicting and Utilizing Dynamic Loop Characteristics. *Proc. ACM*

- Program. Lang.* 7, OOPSLA2, Article 228 (oct 2023), 31 pages. <https://doi.org/10.1145/3622803>
- Wei Niu, Gagan Agrawal, and Bin Ren. 2024. SoD2: Statically Optimizing Dynamic Deep Neural Network. arXiv:2403.00176 [cs.PL]
- Nvidia. 2020a. Nvidia A100 Tensor Core GPU. <https://www.nvidia.com/en-in/data-center/a100/>. [Online; accessed 18-Jan-2024].
- Nvidia. 2020b. Nvidia RTX3080 Tensor Core GPU. <https://www.nvidia.com/en-in/geforce/graphics-cards/30-series/>. [Online; accessed 18-Jan-2024].
- Ookami. 2022. ACCESS Research Provider, A64FX Cluster. <https://www.stonybrook.edu/ookami/>. [Online; accessed 18-Jan-2024].
- Adam Paszke, Sam Gross, Francisco Massa, Adam Lerer, James Bradbury, Gregory Chanan, Trevor Killeen, Zeming Lin, Natalia Gimelshein, Luca Antiga, Alban Desmaison, Andreas Köpf, Edward Yang, Zach DeVito, Martin Raison, Alykhan Tejani, Sasank Chilamkurthy, Benoit Steiner, Lu Fang, Junjie Bai, and Soumith Chintala. 2019. PyTorch: an imperative style, high-performance deep learning library. In *NIPS*. Curran Associates Inc., Red Hook, NY, USA, Article 721, 12 pages.
- Philip Pfaffe, Tobias Grosser, and Martin Tillmann. 2019. Efficient hierarchical online-autotuning: a case study on polyhedral accelerator mapping. In *ICS (Phoenix, Arizona) (ICS '19)*. Association for Computing Machinery, New York, NY, USA, 354–366. <https://doi.org/10.1145/3330345.3330377>
- Jonathan Ragan-Kelley, Connelly Barnes, Andrew Adams, Sylvain Paris, Frédo Durand, and Saman Amarasinghe. 2013. Halide: a language and compiler for optimizing parallelism, locality, and recomputation in image processing pipelines. *SIGPLAN Not.* 48, 6 (jun 2013), 519–530. <https://doi.org/10.1145/2499370.2462176>
- Fabian Ritter and Sebastian Hack. 2024. Explainable Port Mapping Inference with Sparse Performance Counters for AMD’s Zen Architectures. arXiv:2403.16063 [cs.PF]
- Christian Sarofoen, Piotr Bialecki, Jie Jiang, Kevin Stephano, Masaki Kozuki, Neal Vaidya, and Stas Bekman. 2022. Introducing nvFuser, a deep learning compiler for PyTorch. <https://pytorch.org/blog/introducing-nvfuser-a-deep-learning-compiler-for-pytorch/>. [Online; accessed 15-Mar-2024].
- Junru Shao. 2021. [RFC] Meta Schedule (AutoTensorIR). <https://discuss.tvm.apache.org/t/rfc-meta-schedule-autotensorir/10120>.
- Pramod Singh, Avinash Manure, Pramod Singh, and Avinash Manure. 2020. Introduction to tensorflow 2.0. , 24 pages.
- Tyler Sorensen, Sreepathi Pai, and Alastair F. Donaldson. 2019. One Size Doesn’t Fit All: Quantifying Performance Portability of Graph Applications on GPUs. In *IISWC*. IEEE, New York, US, 155–166. <https://doi.org/10.1109/IISWC47752.2019.9042139>
- Sanket Tavarageri, Alexander Heinecke, Sasikanth Avancha, Bharat Kaul, Gagandeep Goyal, and Ramakrishna Upadrasta. 2021. PolyDL: Polyhedral Optimizations for Creation of High-performance DL Primitives. *Transactions on Architecture and Code Optimization* 18, 1, Article 11 (jan 2021), 27 pages. <https://doi.org/10.1145/3433103>
- Nicolas Tollenaere, Guillaume Iooss, Stéphane Pouget, Hugo Brunie, Christophe Guillon, Albert Cohen, P. Sadayappan, and Fabrice Rastello. 2023. Autotuning Convolutions Is Easier Than You Think. *ACM Trans. Archit. Code Optim.* 20, 2, Article 20 (mar 2023), 24 pages. <https://doi.org/10.1145/3570641>
- Konrad Trifunovic, Albert Cohen, David Edelsohn, Feng Li, Tobias Grosser, Harsha Jagasia, Razya Ladelsky, Sebastian Pop, Jan Sjödin, and Ramakrishna Upadrasta. 2010. GRAPHITE Two Years After: First Lessons Learned From Real-World Polyhedral Compilation. In *GROW, HAL*, Pisa, Italy, 17 pages. <https://inria.hal.science/inria-00551516>
- Jaeyeon Won, Charith Mendis, Joel S. Emer, and Saman Amarasinghe. 2023. WACO: Learning Workload-Aware Co-optimization of the Format and Schedule of a Sparse Tensor Program. In *ASPLOS (Vancouver, BC, Canada)*. Association for Computing Machinery, New York, NY, USA, 920–934. <https://doi.org/10.1145/3575693.3575742>
- Stephen J. Wright. 2015. Coordinate Descent Algorithms. *Math. Program.* 151, 1 (jun 2015), 3–34. <https://doi.org/10.1007/s10107-015-0892-3>
- W. Zangwill. 1969. *Nonlinear Programming, A Unified Approach* (1st ed.). Prentice Hall, USA.
- Bojian Zheng, Ziheng Jiang, Cody Hao Yu, Haichen Shen, Joshua Fromm, Yizhi Liu, Yida Wang, Luis Ceze, Tianqi Chen, and Gennady Pekhimenko. 2022. DietCode: Automatic Optimization for Dynamic Tensor Programs. In *MLSys (Vancouver, BC, Canada)*. Marculescu and Chi, New York, NY, USA, 848–863. <https://doi.org/10.1145/3575693.3575702>
- Lianmin Zheng, Chengfan Jia, Minmin Sun, Zhao Wu, Cody Hao Yu, Ameer Haj-Ali, Yida Wang, Jun Yang, Danyang Zhuo, Koushik Sen, Joseph E. Gonzalez, and Ion Stoica. 2020. Anso: Generating High-Performance Tensor Programs for Deep Learning. In *OSDI*. USENIX Association, USA, Article 49, 17 pages.
- Hongyu Zhu, Ruofan Wu, Yijia Diao, Shanbin Ke, Haoyu Li, Chen Zhang, Jilong Xue, Lingxiao Ma, Yuqing Xia, Wei Cui, Fan Yang, Mao Yang, Lidong Zhou, Asaf Cidon, and Gennady Pekhimenko. 2022. ROLLER: Fast and Efficient Tensor Compilation for Deep Learning. In *OSDI*, Marcos K. Aguilera and Hakim Weatherspoon (Eds.). USENIX Association, New York, USA, 233–248. <https://www.usenix.org/conference/osdi22/presentation/zhu>
- Mikhail Zolotukhin. 2021. NNC walkthrough: how PyTorch ops get fused. <https://dev-discuss.pytorch.org/t/nnc-walkthrough-how-pytorch-ops-get-fused/125>. [Online; accessed 15-Mar-2024].